# Spintronic Memristor Based Temperature Sensor Design with CMOS Current Reference

Xiuyuan Bi*, Chao Zhang*, Hai Li*, Yiran Chen† and Robinson E. Pino‡

*Polytechnic Institute of NYU
xbi01@students.poly.edu
hli@poly.edu

†University of Pittsburgh
yic52@pitt.edu

‡Air Force Research Lab
robinson.pino@rl.af.mil

***Abstract*—As the technology scales down, the increased power density brings in significant system reliability issues. Therefore, the temperature monitoring and the induced power management become more and more critical. The thermal fluctuation effects of the recently discovered spintronic memristor make it a promising candidate as a temperature sensing device. In this paper, we carefully analyzed the thermal fluctuations of spintronic memristor and the corresponding design considerations. On top of it, we proposed a temperature sensing circuit design by combining spintronic memristor with the traditional CMOS current reference. Our simulation results show that the proposed design can provide high accuracy of temperature detection within a much smaller footprint compared to the traditional CMOS temperature sensor designs. As magnetic device scales down, the relatively high power consumption is expected to be reduced.**

***Keywords-thermal sensor; memristor; current reference; temperature***

## I. Introduction

As integrated circuit systems become more and more complex with technology scaling down, the continuously increasing power density and working temperature severely degrade the system reliability. The on-chip temperature sensing circuits are needed to monitor the run-time temperature and prevent the malfunction caused by overheating, especially in reliability-critical systems. Compared to the off-chip temperature sensor, the on-chip (built-in) sensors can obtain a much higher sensing accuracy for its close physical location to heat sources.

In the traditional temperature sensors, the key components for temperature detection are p-n junction diode [25] or transistor [17], which have been well studied. BJT transistor is usually favored by designers. The most popular method is utilizing the difference between base-emitter voltages of a substrate BJT transistor to detect temperature changes [18][20]. To make up the non-perfect linearity of BJT transistor, many curvature correction techniques, such as nested-chopping, auto-zeroing, or offset cancellation, have been investigated. The transistor based temperature sensors usually have large area, which significantly limits the utilization and quantity allowed in the systems [16][23][24].

Memristor [1], a newly re-discovered circuit element, has recently received increased attentions from different areas [2]. Spintronic memristor has been proposed based upon spin-torque-induced magnetization motion and spin transport at ferromagnetic junctions. The transient behavior of a spintronic memristor is governed by the torques acting on its free layer magnetization vector, which is significantly impacted by thermal fluctuations. Therefore, the memristance, a.k.a. the resistance value, demonstrates an obvious temperature dependency under certain design configuration [7].

In this paper, we explore the possibility of using spintronic memristor for temperature sensing. The related circuit design considerations have been discussed. On top of it, we propose a temperature sensing circuit design that utilizes spintronic memristor as the sensing device. Benefiting from the unique hysteresis voltage-current property of memristor at finite temperature, the memristance change is used to measure the ambient temperature. A stable CMOS current reference is applied as the stimulus to drive the sensing device. The simple circuit scheme produces a very small sensor area. Furthermore, the opposite temperature dependencies of memristor and current reference compensate each other and produce a fine linearity at the output voltage with respect to temperature.

The paper is organized as follows. In Section II, we will briefly introduce the fundamental of spintronic memristor and its temperature dependency. The design considerations by comparing constant voltage and constant current sources are discussed in Section III. Section IV explains the design concept and demonstrates simulation results. The comparison with the previous temperature sensor designs can be found in Section V. At last, we summarize and conclude the work in Section VI.

## II. Background

### A. Memristor theory

Forty years ago, Professor Chua [1] observed the six different mathematical relations connecting pairs of the four fundamental circuit variables: electric current *I*, voltage *V*, charge *q* and magnetic flux $\varphi$. Accordingly, there should be a fourth basic circuit element, namely, memristor, to complete the relations between those variables. The memristor, with memristance *M*, bridges the electronic charge and magnetic flux as $d\varphi = M \cdot dq$, as shown in Figure 1. The existence of memristor kept unrevealed until 2008 when HP lab firstly discovered it through a $TiO_2$ thin-film structure [2].

Memristors show many promising characteristics as the next-generation data storage devices, such as non-volatility, low-power consumption, high integration density and excellent scalability [3][4].

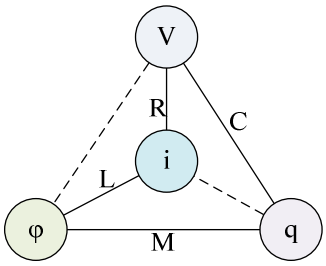


Figure 1. The four fundamental two-terminal circuit elements. The dashed lines represent $\varphi(t) = \int_{t_0}^{t} v(\tau)d\tau$ and $q(t) = \int_{t_0}^{t} i(\tau)d\tau$ equations. *R*, *C*, *L* and *M* are resistor, capacitor, inductor, and memristor, respectively. [1]

978-3-9810801-8-6/DATE12/©2012 EDAA

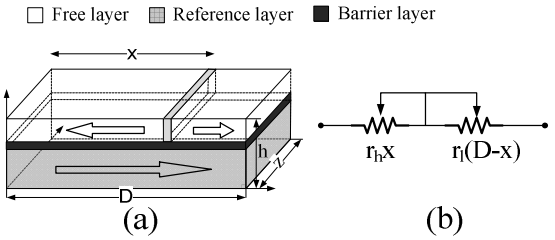


Figure 2. Spintronic memristor: (a) Physical structure. (b) Equivalent circuit.

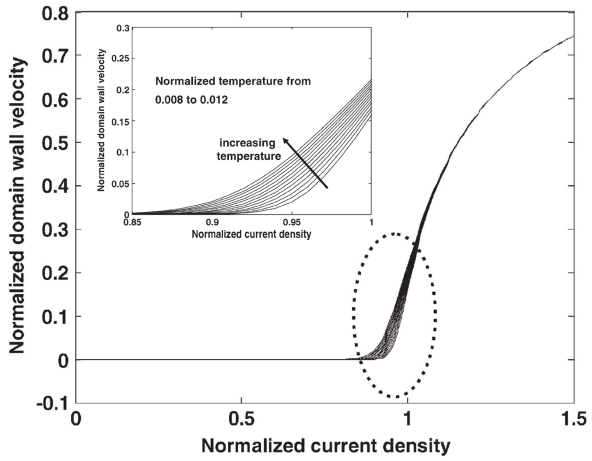


Figure 3. Average domain-wall velocity as a function of the normalized current density for different thermal fluctuation strengths.

Also, the special property that records historical profile of the electrical excitations on the device [5] makes memristor an ideal candidate to realize the synapse behavior in electronic neural networks. In this work, we use memristor as temperature sensor by utilizing its characteristic of temperature dependency.

## B. *Spintronic memristor*

Among various memristor devices, the spintronic memristive device based on giant magneto-resistance (GMR) magnetic tunneling junction (MTJ) is one of the most promising one for its simple structure [6][7]. As illustrated in Figure 2(a), the device is composed of two ferromagnetic layers: reference and free layers. The reference layer is coupled to a pinned magnetic layer and hence has a fixed magnetic direction. The free layer includes two anisotropy segments divided by a domain-wall. The resistance per unit length (resistivity) of each segment is determined by the relative magnetic directions of the free layer and reference layer: when they are parallel, the resistivity is low; otherwise, the resistivity is high.

Figure 2(b) shows the simplified equivalent circuit model of the spintronic memristor. The overall resistance can be modeled as two resistors connected in series:

$$M = r_H \cdot X(t) + r_L \cdot [D - X(t)] \tag{1}$$

where $r_L$ and $r_H$ denote the resistance per unit length when the segment of spin-valve strip is at low- and high-resistance states, respectively. $D$ represents the length of the device. $X(t)$ is the position of domain-wall, which is moved by current-induced spin-torque excitation[1]. It can be calculated by the integral of the domain wall velocity $v$ over time $t$ as:

$$X(t) = \int_0^t v dt = \int_0^t \frac{J \cdot P \cdot \mu_B}{e \cdot M_s} dt \tag{2}$$

where the velocity $v$ is proportional to the current density $J$, which can be calculated as

$$J(t) = \frac{V(t)}{M(t) \cdot h \cdot z} \tag{3}$$

Here, $V(t)$ is the voltage applied to memristor. $h$ and $z$ are the thickness and the width of spin-valve strip, respectively. $P$ is polarization efficiency. $u_B$ is Bohr magneton. $e$ is elementary charge. And $M_S$ is magnetization saturation. The domain wall movement in a spintronic memristor happens only when the current density $J(t)$ is above the critical current density $J_{cr}$ [8][9].

## C. *Temperature dependency*

At a finite temperature, the domain wall velocity $v$ is the derivative of domain wall position $X(t)$, which satisfies the following stochastic differential equations:

$$\frac{d\phi}{dt} + \frac{\alpha}{\omega}\frac{dX}{dt} = \eta_\phi, \text{ and} \tag{4}$$

$$\frac{1}{\omega}\frac{dX}{dt} - \alpha\frac{d\phi}{dt} = \omega_0 \sin(2\phi) + \frac{v}{\omega} + \eta_x \tag{5}$$

Where $\phi$ is the plane angel of domain wall motion. $\omega_0 = \gamma H_p / 2$ ($\gamma$ is the gyro-magnetic ration). $\alpha$ is the damping parameter. $\eta_\phi(t)$ and $\eta_X(t)$ are the $\phi$ and $X$ component thermal fluctuation fields, respectively. Their magnitudes are determined by the fluctuation dissipation condition

$$<\eta_\phi(t) \cdot \eta_\phi(t')> = <\eta_X(t) \cdot \eta_X(t')> = \frac{2ak_BT}{hN}\delta(t-t') \tag{6}$$

where $k_B$ is the Boltzmann constant, $T$ is the temperature, $h$ is the Plank constant, and $n = 2hS/\alpha^3$ is the number of spins in the domain wall with the cross-sectional surface area $S$ and domain-wall thickness $h$. $\alpha$ is the lattice constant.

As in Equation (5), the domain wall velocity $v$ depends on spin torque excitation strength and thermal fluctuation magnitude. The spin torque excitation strength is proportional to current density, which can be normalized as $J_{norm}$. At absolute zero, $J_{norm}$ strictly confines the domain wall motion, as domain wall doesn't move until the current density exceeds the critical value, i.e., when $J_{norm} = 1$. While under some finite temperature, due to thermal fluctuation, the domain wall will start moving even when current density is less than the critical value. Thus the normalized domain wall velocity $v_{norm}$, *i.e.*, the derivative of domain wall position, can be expressed as a function of normalized current density $J_{norm}$ and the normalized thermal fluctuation magnitude $\eta_X$.

TABLE I. CONSTANTS AND PARAMETERS IN MODEL

| | | |
|---|---|---|
| **Physical constants** | | |
| $e$ | Elementary charge (C) | 1.602e-19 |
| $u_B$ | Bohr magnetron (J/T) | 9.274e-24 |
| **Material parameters** | | |
| $H_p$ | Hard anisotropy (Oe) | 5000 |
| $H_k$ | Easy anisotropy (Oe) | 100 |
| $M_s$ | Magnetization saturation (emu/cc) | 1010 |
| $A$ | Exchange parameter (J/m) | 1.8e-11 |
| $\alpha$ | Damping parameter | 0.02 |
| $P$ | Polarization efficiency | 0.3 |
| $\gamma$ | Gyromagnetic ratio | 1.75e7 |
| $J_{cr}$ | Critical current density(A/cm$^2$) | 3·10e8 |
| **Model parameters** | | |
| $D$ | Length (nm) | 268 |
| $h$ | thickness(nm) | 10 |
| $z$ | Width (nm) | 17 |
| $R_{h0}$ | Low sheet resistance (Ω) | 50(when h=70 Å) |
| $GMR$ | Giant magneto resistance ratio | 12% |

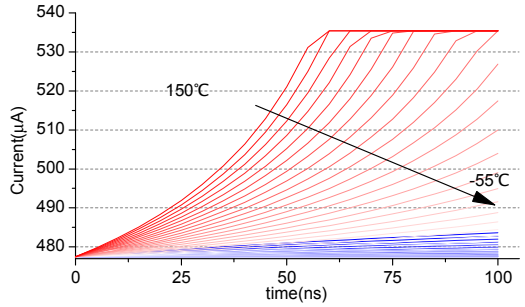


Figure 4. The transient current curves under various temperatures when applying a constant voltage pulse.

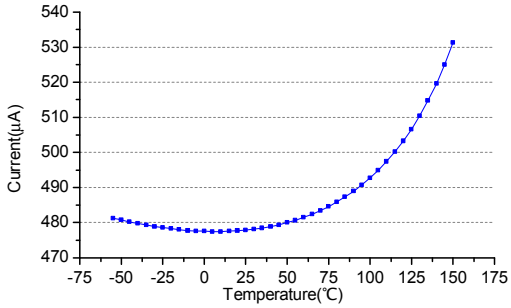


Figure 5. The relationship between the memristor current and the ambient temperature. The sample time is set as 55ns.

TABLE I summarizes the material parameters used in memristor device simulation [12]. The simulated relation between the normalized velocity $v_{norm}$ and the normalized current density $J_{norm}$ is shown in Figure 3. At room temperature T=27°C, the critical current density is $J_{cr}$ = $3\cdot10^8$A/cm$^2$, and the normalized velocity is $v_{norm}$ =52m/s. Around the critical current density zone, the curves vary with thermal fluctuation magnitude. Temperature sensitive and insensitive regions can be observed.

With high current density, the velocity variations magnitude becomes bigger, where the velocity-current curves in various temperatures separated from each other. Around critical current density, the velocity variation is most significant, and when the current keeps increasing, the bundle of curves gradually become close to each other. Physically, under a certain electrical field which can provide strong enough pushing strength to the domain wall, the temperature effect can be ignored. Therefore in the proposed spintronic memristor temperature sensor design, we constrain the design within this thermal sensitive region.

## III. Design Considerations

In order to get an insight of memristor thermal property, we investigate two methods – the constant voltage driving and the constant current driving, to explore the trend of memristance changes. In each test, we initialize the domain wall at the highest memristance state, and move it toward the lowest memristance state. A higher temperature will result in an increased domain-wall motion, which leads to a smaller memristance.

### *A. Constant voltage driving*

When a constant voltage pulse is applied to the two terminals of a memristor, the reduced memristance can result in a higher driving current density. This positive feedback procedure accelerates the domain-wall movement and enhances the memristance reduction.

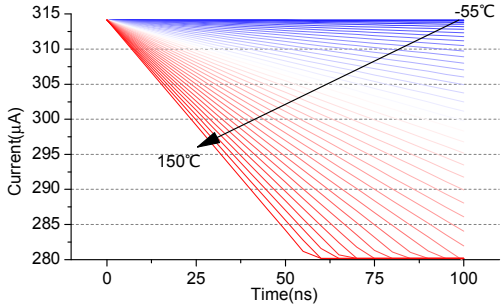


Figure 6. The transient voltage curves under various temperatures.

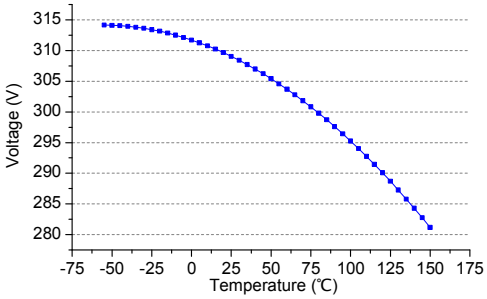


Figure 7. The relationship between the memristor voltage and the ambient temperature. The sample time is set as 55ns.

In the experiment, we provide a stable voltage source with 0.3V amplitude. Initially, the domain wall starts at the highest memristance end. Since $X(t)$ is the time integral of domain-wall velocity, the differential equation can be modified as:

$$(r_H - r_L)\cdot v = \frac{V}{I(t)^2}\cdot\frac{dI(t)}{dt} \tag{7}$$

Figure 4 shows the simulated transient currents under various temperatures. As expected, at a higher temperature, the current through the spintronic memristor rises faster. The positive feedback also contributes to the kneeling shape of the transient curves, at which the domain wall reaches the other end. When the pulse width is around 55ns, those current curves under different temperatures demonstrate the biggest difference. Hence, we set the pulse width as 55ns and detect the current through the memristor. The relationship of current and ambient current is shown in Figure 5.

### *B. Constant current driving*

When using the current source as a constant drive, the domain wall velocity can be obtained by

$$-(r_H - r_L)\cdot v = \frac{dV(t)}{I\cdot dt} \tag{8}$$

Here, the current $I$ is constant, and hence, the domain wall velocity $v$ is fixed. Therefore, the voltage cross the memristor decreases linearly, providing a nice linearity curve for temperature detection. When constraining the current density through the memristor close to $J_{norm}$, the difference of voltage across the memristor under the different temperatures can be maximized. The corresponding simulation result is shown in Figure 6.

Similarly, we set the current pulse width as 55ns and sample the voltage across the memristor. The temperature sweep curve is shown in Figure 7. We have observed that the voltage transient curve in Figure 7 has a much better linearity than that in Figure 5. Thus, the fixed current driving is preferred in the design.

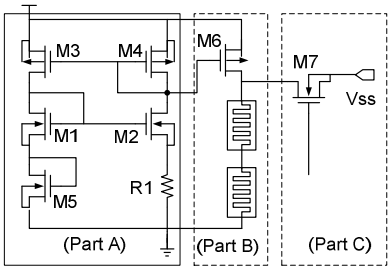


Figure 8. The design diagram of the memristor based temperature sensor.

TABLE II. PARAMETERS OF THE PROPOSED DESIGN

| Physical Parameters | | |
|---|---|---|
| M1/2 | nMOS | W/L=1.8u/90n |
| M3/4 | pMOS | W/L=3.6u/90n |
| M5 | nMOS | W/L=720n/90n |
| M6 | pMOS | W/L=1.8u/90n |
| R1 | Doped Poly-silicon | 9.5KΩ |

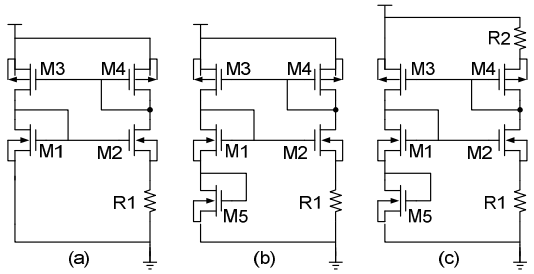


Figure 9. Current reference designs. (a) Design 1: the typical current reference. (b) Design 2: with the first-order temperature compensation. (c) Design 3: with the second-order temperature compensation.

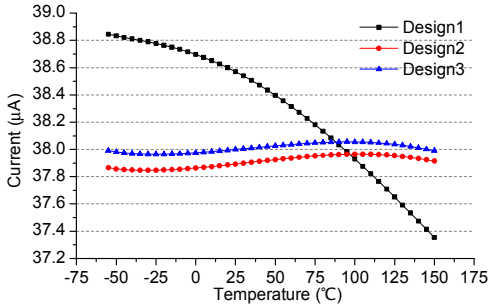


Figure 10. The comparison of temperature sensitivity for the three current reference designs in Figure 9

## IV. CIRCUIT DESIGN AND EXPERIMENTS

### A. Circuit scheme

Figure 8 illustrates the diagram of the spintronic memristor based temperature sensor design, which includes three function modules. *Part A* is used to generate current reference. It consists of a modified NMOS Widlar current mirror $M_1$-$M_2$-$M_5$-$R_1$ and an inverse PMOS Widlar current mirror $M_3$-$M_4$ [10]. The left and right branches balance the current flow with compensation of the diode-connected $M_5$ and the resistor $R_1$. The current reference can be well constraint within 1μA fluctuation. *Part B* is the driving circuit. The PMOS current mirror $M_4$-$M_6$ copies the current reference to drive the memristor. The domain wall is initially set at the upper boundary of the device with the maximized memristance. *Part C* is the detect/reset mode control switch, which determines the driving pulse width and temperature detection. With $M_7$ on and off, the driving circuit switches between detect mode and reset mode. We use a negative power supply $V_{SS}$ to reset the status of memristor by applying an inverse current flow.

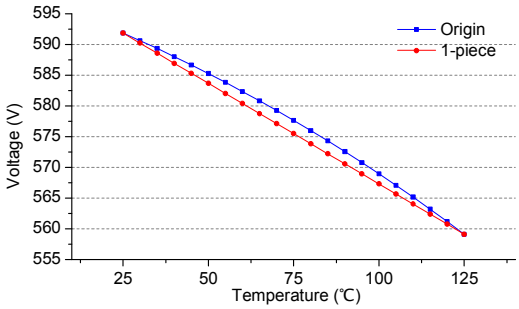


Figure 11. The voltage-temperature curve and the linear fitting function.

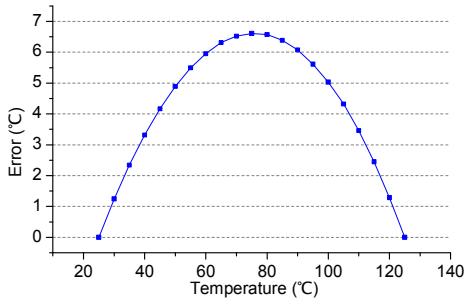


Figure12. Error distribution by using the linear fitting function.

TABLE II summarizes the design parameters of the scheme in Figure 8. Here, 90nm PTM model [11] was used in the design and the following simulations. The power supply $V_{DD}$ is set to 1.0V. All the simulations were conducted in Cadence design environment.

### B. Current reference design

According to the preliminary analysis on temperature sensitivity of spintronic memristor in Section III, a constant current source can obtain a better linearity at voltage output as the temperature sweeps. Here, we compare and evaluate three temperature compensation current reference designs: the typical current reference, the first-order and the second-order temperature compensation current reference. The corresponding circuit diagrams are illustrated in Figure 9 [10]. Figure 10 compares the temperature sweep simulation results of the three designs. The simulation includes the impacts of the temperature sensitive terms in transistors, such as thermal drift effects of electron/hole mobility, thermal resistance effect and threshold voltage.

By comprehensively considering the stability of current source and the design complexity, we use "design2" with the first-order temperature compensation to generate the current reference in our design.

### C. Driving mechanism

By simply adding a PMOS transistor $M_6$, the current reference is mirrored to drive the memristor based sensing device. The size of PMOS $M_6$ should be carefully tuned to constraint the memristor current within temperature sensitive range according to the device analysis in Section II. In order to enlarge the output voltage range, we use two memristor connected in series as the load, as shown in Figure 8. Double the length of the spin-valve strip can result in the same overall memristance. However, the switching time to achieve the same output voltage change is also doubled.

When the design is in the detect mode, the domain wall of the memristor is pushed toward the low memristance end in a steady velocity by the constant current driving. Therefore, the output voltage is a monotone decreasing linear function. Once the domain wall hits the other end, the output voltage flattens out. In Figure 11, we plot the output voltage by sweeping the temperature. We notice that the voltage-temperature curve of memristor in Figure 7 doesn't have good

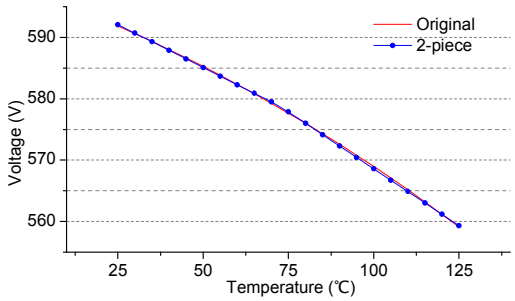


Figure 13. The voltage-temperature curve and the 2-segment piecewise fitting function.

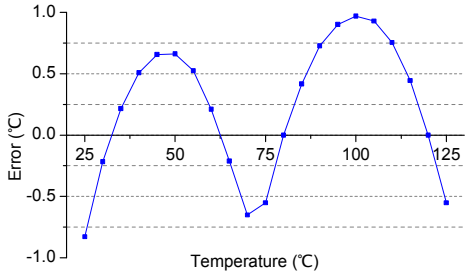


Figure14. Error distribution by using the 2-segment piecewise fitting function.

linearity. It has a little twisted shape with a positive curvature at the low temperature range. Luckily, the current-temperature relation of "Design 2" has the opposite curvature (see Figure 10). The two effects compensate each other and result in a better voltage-temperature linearity in the proposed temperature sensor design, as shown in Figure 11.

A look-up table is usually used to reflect the relationship between the temperature changes and the probed output voltage linear variation. First, we try a linear function to fit the output voltage vs. temperature. Figure 11 shows the fitting curve, and Figure 12 demonstrates the corresponding error distribution. The biggest error rate happens around 70°C because the current flow generated by the reference circuit changes faster than the resistance drops as temperature changes.

Limited by the design scheme, the linearity of the voltage-temperature curve can hardly be improved. Therefore, we tend to use mathematic method to calibrate the look-up table. By observing that the greatest curvature happens around 70°C, we break the temperature range into two pieces: 25°C to 70°C, and 70°C to 125°C. The fitting curve and the corresponding error resolution analysis are shown in Figure 13 and Figure 14, respectively. Compared to the one-piece linear fitting attempt in Figure 13, the two-segment piecewise function fits better with the original sensor output curve. The error resolution is controlled in the range of –0.9 °C to +0.9 °C.

### *D. Process variation considerations and calibrations*

Due to the relentless scaling of CMOS technology, the process variations can dramatically impact the temperature sensor design [13]. Besides the lithographic variations, the aggressive scaling also brought in many non-lithographic sources of variations, such as the dopant variation, well-proximity effects, layout dependent stress variation, rapid thermal anneal temperature induced variation, etc. Fortunately, all these variations can be characterized and modeled to improve model-to-hardware correlation [14]. Here, we run corner simulations by using PTM 90nm corner models [11] to analyze the impacts of process variations.

The simulations at five corners "TT", "SS", "FF", "SF", and "FS", have been investigated. In each setup, the first and second letters

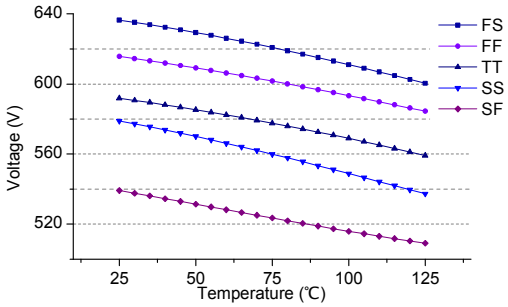


Figure 15. The voltage-temperature curve at five different corners.

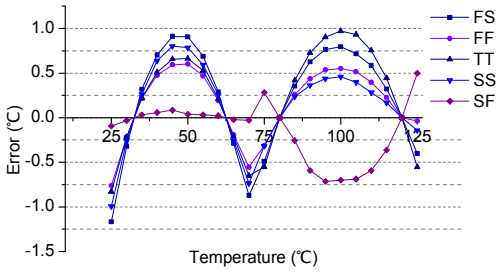


Figure 16. Error distribution by using the 2-segment piecewise fitting function at five different corners.

represent the corner models of NMOS and PMOS transistors, respectively. Each transistor type has three corners: Typical (T), Slow (S), and Fast (F). The voltage-temperature curves and the corresponding error distributions by using the 2-segment piecewise fitting function are demonstrated in Figure 15 and Figure 16, respectively.

The process variations affect the current through memristor and hence the domain wall motion. Therefore, the domain wall velocity varies under the different circumstances. In order to obtain the biggest output voltage differences when varying temperatures, the sample time should always be set close to the flatten-out point of the fastest voltage changing curve at 125°C. The post-fabrication testing is essential to control the sensitivity of this thermal sensor design. Based on the testing data, we shall setup the sampling time and calibrate the look-up table.

### *E. Detecting and resetting*

In on-chip temperature detection, the sensor switches between detect mode and reset mode, determined by the required working frequency. In detect mode, the memristor-based sensing device is driven by the current source and the output voltage is extracted to feed to the thermal management modules. Once detection is completed, we need reset the sensing device to the initial state. As the case of memristor-based sensing design, the domain-wall must be pushed back to the starting point at which the device has the highest memristance. In this design, we implement a track/hold switch to control the detecting and resetting [15].

As shown in Figure 8, an NMOS transistor $M_7$ is used as the switch. When $M_7$ is turned off, the proposed temperature design enters the detect mode. A negative power supply $V_{SS}$ is supplied when $M_7$ is turned on and the circuit is in reset mode. A current flows from memristors to $M_7$. The memristance is reset to high resistant sate by the "inversed" current flow. A periodic voltage pulse can be applied to the gate of $M_7$ to manage operation of the temperature sensor. Based on our previous discussion, the sensor can works at a working frequency of 10MHz.

TABLE III COMPARISON OF DIFFERENT TEMPERATURE SENSORS

| Sensor | power | Temperature range | Inaccuracy (error) | Sensor Type | Process | Linearity | Area |
|---|---|---|---|---|---|---|---|
| [16] | 25uW | 50 ~ 125 °C | -1.0 ~ +0.8 °C | 4 Tr, Analog Voltage | 90nm CMOS | -1.8mV/1 °C | 11.6x4.1um$^2$ |
| [17] | 100uW | 10 ~ 100 °C | ±1°C | 3 Tr, current output | 1.0um CMOS | 0.74%/1 °C | 0.0028mm$^2$ |
| [18] | 1uW | -55 ~ 125 °C | ±1°C | Calc. DVBE | 0.65um CMOS | | 3.32 mm$^2$ |
| [19] | | 20 ~ 110 °C | | MOS tunneling | | 2V/°C | 2.5x2.5mm$^2$ |
| [20] | 429uW | -50 ~ 125 °C | ±0.5°C | Calc. DVBE | 0.5um CMOS | | 2.5 mm$^2$ |
| [21] | 10uW | 0 ~ 100 °C | -0.7 ~ +0.9 °C | temp.-to-pulse | 0.35um CMOS | | 0.175mm$^2$ |
| [22] | 96nW | 25 ~ 97 °C | ±0.25°C | u and Vth intercept | 0.5um CMOS | 0.5mV/°C | 64.8um$^2$ |
| [23] | 1095uW | -30 ~ 90 °C | -0.8 | Calc. DVBE | 0.18um CMOS | | 0.08mm$^2$ |
| [24] | | -60 ~ 140 °C | | Calc. DVGS | 0.18um CMOS | | 0.00126mm$^2$ |
| This work | 400uW | 27 ~ 127 °C | ±1°C | Spintronic memristor | 90nm CMOS+Mag | 0.538mV/°C | 3.0x4.3um$^2$ |

## V. COMPARISON WITH PREVIOUS DESIGNS

The comparison of the proposed memristor-based temperature sensing circuit design and some previous works are summarized in TABLE III. By using the memristor, the design complexity can be significantly reduced, which leads to a small area. The proposed design also demonstrates a fine linearity with respect to temperature changes. The relative high power consumption is due to the required current density through the spintronic memristor. Since the critical current density is proportional to its cross-sectional surface area, this issue is expected to alleviated as technology scales down.

## VI. CONCLUSION AND FUTURE WORK

In this paper, we combine the emerging spintronic memristor and the traditional CMOS current reference to conduct a novel temperature sensing circuit design with high detection accuracy and small footprint. The proposed design shows a high linearity of output voltage, i.e., 0.538mV/°C because the curvature of memristor and the out-coming current can cancel each other coincidentally in a reluctant way. For the simple design scheme, the proposed structure can significantly reduce the area of temperature sensor, and hence, has a great potential in on-chip systems. At last, we analyze the impacts of process variations. A post-fabrication calibration is needed for the proposed design to obtain the required temperature detection accuracy.

## REFERENCES


[1] L. Chua, "Memristor-the missing circuit element," IEEE Trans. on Circuit Theory, vol. 18, pp. 507-519, 1971.

[2] D. B. Strukov, et al., "The missing memristor found," Nature, vol. 453, pp. 80-83, 2008.

[3] D. Niu, Y. Chen, C. Xu, and Y. Xie, "Impact of process variations on emerging memristor," In Design Automation Conference (DAC), pages 877–882, 2010.

[4] Y. Ho, G. M. Huang, and P. Li, "Nonvolatile memristor memory: device characteristics and design implications," In International Conference on Computer-Aided Design, pages 485–490, 2009.

[5] D. Strukov, J. Borghetti, and S. Williams, "Coupled ionic and electronic transport model of thin-film semiconductor memristive behavior," SMALL, 5:1058–1063, 2009.

[6] X. Wang, Y. Chen, H. Xi, H. Li and D. Dimitrov, "Spintronic Memristor Through Spin-Torque-Induced Magnetization Motion," *IEEE Electron Device Letters*, vol.30, no.3, pp.294-297, 2009.

[7] X. Wang, Y. Chen, Y. Gu, and H. Li, "Spintronic Memristor Temperature Sensor," *IEEE Electron Device Letters*, vol. 31, no. 1, January 2010, pp. 20-22.

[8] Z. Li and S. Zhang, "Domain-wall dynamics driven by adiabatic spin-transfer torques," *Physicas Review B*, vol. 70, pp.024417, 2004.

[9] G. Tatara and H. Kohno, "Theory of current-driven domain wall motion: spin transfer versus momentum transfer," *Physicas Review B*, vol. 92, pp. 086601, 2004.

[10] F. Fiori and P. S. Crovetti, "A new compact temperature-compensated CMOS current reference," *IEEE Transactions on Circuits and Systems II*, vol.52, no.11, pp. 724- 728, Nov. 2005.

[11] Y. Cao and et. al. "New paradigm of predictive mosfet and interconnect modeling for early circuit design," In IEEE Custom Integrated Ckt. Conf., pages 201–204, 2000. http://www-device.eecs.berkeley.edu/ptm.

[12] Y. Chen and X. Wang, "Compact modeling and corner analysis of spintronic memristor," *IEEE/ACM International Symposium on Nanoscale Architectures*, pp.7-12, 2009.

[13] W. Zhao, Y. Cao, F. Liu, K. Agarwal, D. Acharyya, S. Nassif, and K. Nowka, "Rigorous extraction of process variations for 65nm CMOS design," *European Solid State Circuits Conference*, pp.89-92, 2007.

[14] K. Agarwal and S. Nassif, "Characterizing Process Variation in Nanometer CMOS," *ACM/IEEE Design Automation Conference (DAC)*, pp.396-399, 2007.

[15] B. Datta, W. Burleson, "Low-power, process-variation tolerant on-chip thermal monitoring using track and hold based thermal sensors," *ACM Great Lakes symposium on VLSI (GLSVLSI)*, pp.145-148, 2009.

[16] M. Sasaki, M. Ikeda, K. Asada, "A Temperature Sensor With an Inaccuracy of -1.0/ +0.8 °C Using 90-nm 1-V CMOS for Online Thermal Monitoring of VLSI Circuits," IEEE Transactions on Semiconductor Manufacturing , vol.21, no.2, pp.201-208, 2008.

[17] V. Szekely, C. Marta, Z. Kohari, M. Rencz, "CMOS sensors for on-line thermal monitoring of VLSI circuits," IEEE Transactions on Very Large Scale Integration (VLSI) Systems, vol.5, no.3, pp.270-276, 1997.

[18] M. Tuthill, "A switched-current, switched-capacitor temperature sensor in 0.6-µm CMOS," IEEE Journal of Solid-State Circuits, vol.33, no.7, pp.1117-1122, Jul 1998.

[19] Y. Shih, S. Lin, T. Wang, J. Hwu , "High sensitive and wide detecting range MOS tunneling temperature sensors for on-chip temperature detection," IEEE Transactions on Electron Devices, vol.51, no.9, pp. 1514- 1521, 2004.

[20] M.A.P. Pertijs, K.A.A. Makinwa, J.H. Huijsing, "A CMOS smart temperature sensor with a 3σ inaccuracy of ±0.1°C from -55°C to 125°C," IEEE Journal of Solid-State Circuits, vol.40, no.12, pp. 2805-2815, 2005.

[21] P. Chen, C. Chen, C. Tsai, W. Lu, "A time-to-digital-converter-based CMOS smart temperature sensor," IEEE Journal of Solid-State Circuits, vol.40, no.8, pp. 1642- 1648, 2005.

[22] Y. Zhai, S.B. Prakash, M.H. Cohen, P.A. Abshire, "Detection of on-chip temperature gradient using a 1.5V low power CMOS temperature sensor," IEEE International Symposium on Circuits and Systems, pp.1171-1174, 2006.

[23] D. Han, Y. Kwon, T. Park, H. Park , "A CMOS temperature sensor with calibration function using band gap voltage reference," International Conference on Sensing Technology, pp.496-499, 2008.

[24] J.T. Tsai, H. Chiueh, "High linear voltage references for on-chip CMOS smart temperature sensor from −60°C to 140°C," IEEE International Symposium on Circuits and Systems, pp.2689-2692, 2008.

[25] G. Fisher, J. C. Daly, C. W. Recksiek, K. D. Friedland, "A programmable temperature monitoring device for tagging small fish: A Prototype Chip Development," IEEE Transactions on Very Large Scale Integration (VLSI) System., vol. 5, pp. 401–407, 1997.